The Illumination Intensity and Applied Bias Voltage on Dielectric Properties of Au/Polyvinyl Alcohol (Co, Zn-Doped)/n-Si Schottky Barrier Diodes

Habibe Uslu,[1] Şemsettin Altındal,[1] Tuncay Tunç,[2] İbrahim Uslu,[3] Tofig S. Mammadov[1,4]

[1]*Department of Physics, Faculty of Science and Arts, Gazi University, Ankara, Turkey*
[2]*Science Education Department, Faculty of Education, Aksaray University, Aksaray, Turkey*
[3]*Department of Chemistry Education, Selçuk University, Konya, Turkey*
[4]*Department of Nano Technology, National Academy of Science, Institute of Physics, Baku, Azerbaijan*

Received 16 April 2010; accepted 2 August 2010
DOI 10.1002/app.33131
Published online 13 October 2010 in Wiley Online Library (wileyonlinelibrary.com).

ABSTRACT: The Au/polyvinyl alcohol (PVA) (Co, Zn-doped)/n-Si Schottky barrier diodes (SBDs) were exposed to various illumination intensities. Illumination effect on the dielectric properties has been investigated by using capacitance–voltage (C–V) and conductance–voltage (G/ω–V) characteristics at 1 MHz and room temperature. The values of dielectric constant (ε'), dielectric loss (ε''), loss tangent ($\tan\delta$), electric modulus (M' and M''), and AC electrical conductivity (σ_{AC}) were found strongly intensity dependent on both the illumination levels and applied bias voltage especially in depletion and accumulation regions. Such bias and illumination dependency of these parameters can be explained on the basis of Maxwell–Wagner interfacial polarization and restructuring and reordering of charges at interface states. In addition, the ε'–V plots also show an intersection feature at $\sim$ 2.8 V and such behavior of the ε'–V plots appears as an abnormality compared with the conventional behavior of an ideal SBD. The obtained results revealed that illumination intensity enhances the conductivity of Au/PVA(Co, Zn-doped)/n-Si SBD. © 2010 Wiley Periodicals, Inc. J Appl Polym Sci 120: 322–328, 2011

Key words: PVA; illumination effect; voltage dependent; dielectric properties; AC electrical conductivity

INTRODUCTION

Polyvinyl alcohol (PVA) is the most interesting material in view of its large scale electronic application and optoelectronic application. A metal such as cobalt (Co), nickel (Ni), and zinc (Zn) doped PVA films causes improvement of the polymer behavior and often even brings about a progress in performance. Recently, illumination intensity has become one of the most common process producing modifications in their morphological structures, electronic, optoelectronic, and dielectric properties.[1–6] The existence of interfacial layer like insulator or organic materials makes them rather sensitive to illumination intensity. The performance of Schottky barrier diodes (SBDs) and solar cells is drastically influenced by the quality of interfacial layer between the metal and semiconductor surface. In general, considering the performance of these devices, there are several effects that cause deviations of the ideal behavior, and, therefore, they must be taken into account. These include the effects of interfacial layer, interface states (N_{ss}), and the barrier homogeneity at metal/semiconductor (M/S) interface, series resistance (R_s) of device, and fabrication process. Photodiode based on metal-semiconductor SBDs can be fabricated by using different organic semiconductors. When these devices, with an organic interfacial layer, are illuminated, electron-hole pairs are produced so that these devices show photovoltaic feature. Organic materials have a wide application in the thin film electronics because of their low cost production, low molecular weight, and their being produced easily compared with conventional inorganic based technologies. They can be produced in large quantities by simple methods like spin coating, which lowers the production cost.[7]

There are many reports about conjugated conducting polymers on the area of electronic and optoelectronic. Among the various conducting polymers, polyvinyl alcohol, polyaniline, poly (alkylthiophene), polypyrrole, polyophene, and poly (3-hexylthiophene) became an attractive research topic to chemists, physicists, and electrical engineers alike because of their potential applications and interesting properties.[5,8–11] In addition, there are many reports in the literature on PVA based electronic devices and their electric, optic, and dielectric properties as a function of frequency and temperature.[1–16] However, there are few studies on the electrical and dielectric properties and AC electrical conductivity (σ_{AC}) under

Correspondence to: H. Uslu (h.uslu@gazi.edu.tr).

Journal of Applied Polymer Science, Vol. 120, 322–328 (2011)
© 2010 Wiley Periodicals, Inc.

various illumination conditions.[17,18] Therefore, in this study, PVA film was used as an interfacial layer between metal and semiconductor. PVA doped with different ratios of Co and Zn was produced and PVA/(Co, Zn) nanofiber film on silicon semiconductor was fabricated with the use of electrospinning technique. Diffusion of the dopant into the polymer matrix plays an important role in the conduction process. If the dopants are not distributed homogenously to electron donor sites, it will cause partial ionization, and heterogeneity would create small conducting domains separated by some insulating regions of undoped polymer in such a segment rather than by hopping between localized states.[1,6]

Dielectric measurements of these devices such as dielectric constant (ε′), dielectric loss (ε″), loss tangent (tanδ), and AC electrical conductivity (σ_{AC}) are drastically affected by the presence a dopant or dopants in the polymer.[19–21] Also, changes in these parameters with frequency and temperature in the dark is considerably different than the ones under illumination intensity. Under illumination, an excess capacitance can occur because of illumination induced interface states, and it leads to an increase in the real capacitance of structures. Therefore, it is important to include the effect of illumination intensity and bias voltage in the investigation of both electrical and dielectric properties.[22,23] Devices response to illumination in terms of dielectric constant (ε′), dielectric loss (ε″), and loss tangent (tanδ) becomes distinct under high illumination levels.

In this study, Au/PVA (Co, Zn-doped)n-Si SBDs were first fabricated and then both the forward and reverse bias admittance measurements (*C*–*V* and $G/\omega-V$) were studied under various illumination intensities at 1 MHz and −6 to 5 V, respectively, by using an HP-4192A impedance analyzer at room temperature. The variation of ε′, ε″, tanδ, σ_{AC}, and real and imaginary part of electric modulus (*M*′ and *M*″) have been investigated under various illumination intensities.

EXPERIMENTAL PROCEDURE

The Au/PVA (Co, Zn-doped)/n-Si SBDs were fabricated on the 2 inch (5.08 cm) diameter flat zone (111) n-type (phosphor doped) single crystal Si wafer having thickness of 350 μm with ≅0.7 Ω cm. For the fabrication process, the n-type Si wafer was first cleaned in a mixture of a peroxide–ammonia solution and then in H_2O + HCl solution for 10 min and subsequently quenched in deionized water of resistivity of 18 MΩ cm for 15 min. After the cleaning process, high purity Au metal (999.999 %) with a thickness of about 2000 Å was thermally evaporated onto the whole back side of Si wafer at a pressure of $\sim 10^{-6}$ Torr in high vacuum system. To perform a low resistivity ohmic back contact, Si wafer was sintered at 450°C for 5 min in N_2 atmosphere.

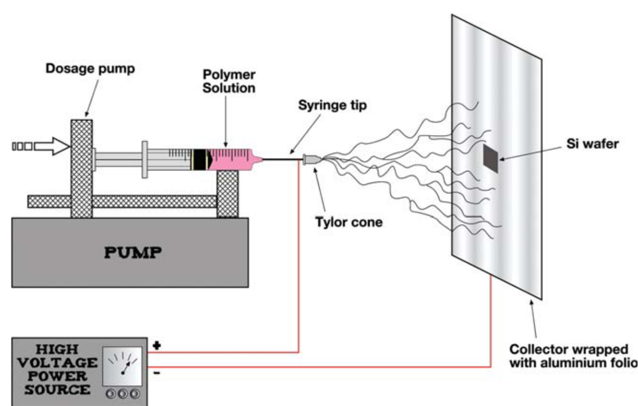

Figure 1 The schematic representation of the electrospinning process. [Color figure can be viewed in the online issue, which is available at wileyonlinelibrary.com.]

The PVA film was fabricated on n-type Si by electrospinning technique. A simple illustration of the electrospinning system is given in Figure 1. Cobalt acetate (0.5 g) and zinc acetate (0.25 g) were mixed with PVA (1 g), molecular weight = 72 000, and 9 mL of deionized water. After vigorous stirring for 2 h at 50°C, a viscous solution of PVA/(Co, Zn-dopped) acetates was obtained.

Using a peristaltic syringe pump, the precursor solution was delivered to a metal needle syringe (10 mL) with an inner diameter of 0.9 mm at a constant flow rate of 0.02 mL/h. The needle was connected to a high-voltage power supply and positioned vertically on a clamp. A piece of flat aluminum foil was placed 15 cm below the tip of the needle to collect the nanofibers. Si wafer was placed on the aluminum foil. On applying a high-voltage of 20 kV on the needle, a fluid jet was ejected from the tip. The solvent evaporated and a charged fiber was deposited onto the Si wafer as a nonwoven mat. After spinning process, circular dots of 1 mm in diameter and 1500 Å thick high purity Au rectifying contacts were deposited on the PVA surface of the wafer through a metal shadow mask in liquid nitrogen trapped oil-free ultra-high vacuum system in the pressure of $\sim 10^{-7}$ Torr. The structure of Au/PVA (Co, Zn-doped)/n-Si SBDs and details of the fabrication process have been given in our previous study.[5]

The *C*–*V* and *G*/ω–*V* measurements were performed in dark and under various illumination intensities at 1 MHz and room temperature by using a HP-4192A LF impedance analyzer and small sinusoidal test signal of 20 $mV_{p\text{-}p}$ from the external pulse generator is applied to the sample to meet the requirement. All measurements were carried out with the help of a microcomputer through an IEEE-488 AC/DC converter card. For illuminating the sample, a 250-W solar simulator (Model: 69931,

Newport-Oriel Instruments, Stratford, CT) was used as a light source. The photons at different power levels passed through an AM1.5 filter that allows wavelengths only between 400 and 700 nm and reaches the surface of the diodes. The intensity of the light was measured by research radiometer (Model ILT1700, International Light Technologies, MA).

RESULTS AND DISCUSSION

The illumination intensity and applied bias voltage dependence of dielectric constant (ε'), dielectric loss (ε''), loss tangent (tanδ), AC electrical conductivity (σ_{AC}), and real and imaginary parts of electric modulus (M' and M'') were evaluated from the data gathered from C–V and G/ω measurements of Au/PVA (Co, Zn-doped)n-Si SBDs in the illumination range of 50–250 W at 1 MHz and at room temperature. To describe the dielectric properties and AC electrical conductivity of the structure, complex permittivity is defined as[24–28]:

$$\varepsilon^* = \varepsilon' - i\varepsilon'' \quad (1)$$

where ε' and ε'' are the real and imaginary parts of complex permittivity, respectively, and i is the imaginary root of -1. The complex permittivity formalism has been employed to describe the electrical and dielectric properties. In the ε^* formalism, in the case of admittance Y^* measurements, the following relation holds:

$$\varepsilon^* = \frac{Y^*}{i\omega C_o} = \frac{C}{C_o} - i\frac{G}{\omega C_{o_i}} \quad (2)$$

where C and G are the measured capacitance and conductance values of the polymer material, respectively, and ω is the angular frequency ($\omega = 2\pi f$) of the applied electric field.

The dielectric constant (ε') which is the real part of the complex permittivity is calculated at the various illumination intensities by using the measured C values for each bias voltage from the relation[22,29]:

$$\varepsilon' = \frac{C}{C_o} = \frac{Cd}{\varepsilon_o A} \quad (3)$$

where $C_o = \varepsilon_o A/d$ is capacitance of an empty capacitor, A is the rectifier contact area of the structure in cm^2, d is the interfacial polymer layer thickness, and ε_o is the electric permittivity of free space ($\varepsilon_o = 8.85 \times 10^{-14}$ F/cm). In the strong accumulation region, the maximal capacitance of the metal-insulator-semiconductor (MIS) capacitance corresponds to the interfacial polymer capacitance ($C_o = \varepsilon' C_o = \varepsilon' \varepsilon_o A/d$). The dielectric loss ($\varepsilon''$), which is the imaginary part of the complex permittivity, is calculated at various illumination intensities by using the measured C values for each bias voltage from the relation[22,29]:

$$\varepsilon'' = \frac{G}{\omega C_o} = \frac{Gd}{\varepsilon_o \omega A} = \varepsilon' \tan\delta \quad (4)$$

where the loss tangent (tanδ) of the polymer as dielectric material is denoted by tanδ and can be expressed as follows[24,30,31]:

$$\tan\delta = \frac{\varepsilon''}{\varepsilon'} \quad (5)$$

The AC electrical conductivity (σ_{AC}) of the dielectric material can be given by the following equation[24,30]:

$$\sigma_{ac} = \omega C \tan\delta (d/A) = \varepsilon'' \omega \varepsilon_o \quad (6)$$

The terms complex impedance (Z^*) and complex electric modulus (M^*) formalisms with regard to the analysis of the dielectric or polymer materials have been discussed by several authors so far, most of whom have preferred electric modulus in defining the dielectric property and conduction mechanism of these materials.[26,31] The data regarding Z^* or the complex dielectric permittivity ($\varepsilon^* = 1/M^*$) data can be transformed into the M^* formalism using the following relation[31–33]:

$$M^* = \frac{1}{\varepsilon^*} = M' + iM'' = \frac{\varepsilon'}{\varepsilon'^2 + \varepsilon''^2} + i\frac{\varepsilon''}{\varepsilon'^2 + \varepsilon''^2} \quad (7)$$

where the real component M' and the imaginary component M'' are calculated from ε' and ε'', respectively. The ε^* and the M* representation allows us to distinguish the local dielectric relation. Generally, to extract as much information as possible, dielectric relation spectroscopy data are used in the electric modulus formalism introduced by Macedo et al.[32] Also, the determination of the electric modulus of these materials and their variation with applied bias voltage provide valuable information that allows study of the relaxation process for a specific electronic application.[28,32,33]

Figure 2(a–c) shows the applied bias voltage dependency of the dielectric parameters, i.e., ε', ε'', and tanδ of Au/PVA (Co, Zn-doped)n-Si SBDs in dark and under various illumination conditions at 1 MHz. As it can be seen in these figures, the values of ε', ε'', and tanδ are strongly dependent on both illumination intensity and applied bias voltage especially in the depletion and accumulation regions. The ε'–V and the ε''–V plots have a peak at about 1.5 V and the magnitude of the peak values of ε' and ε'' increases with the increasing illumination intensity. It is clear that Figure 2(a) shows an interesting characteristic of the forward bias ε'–V plot that is the

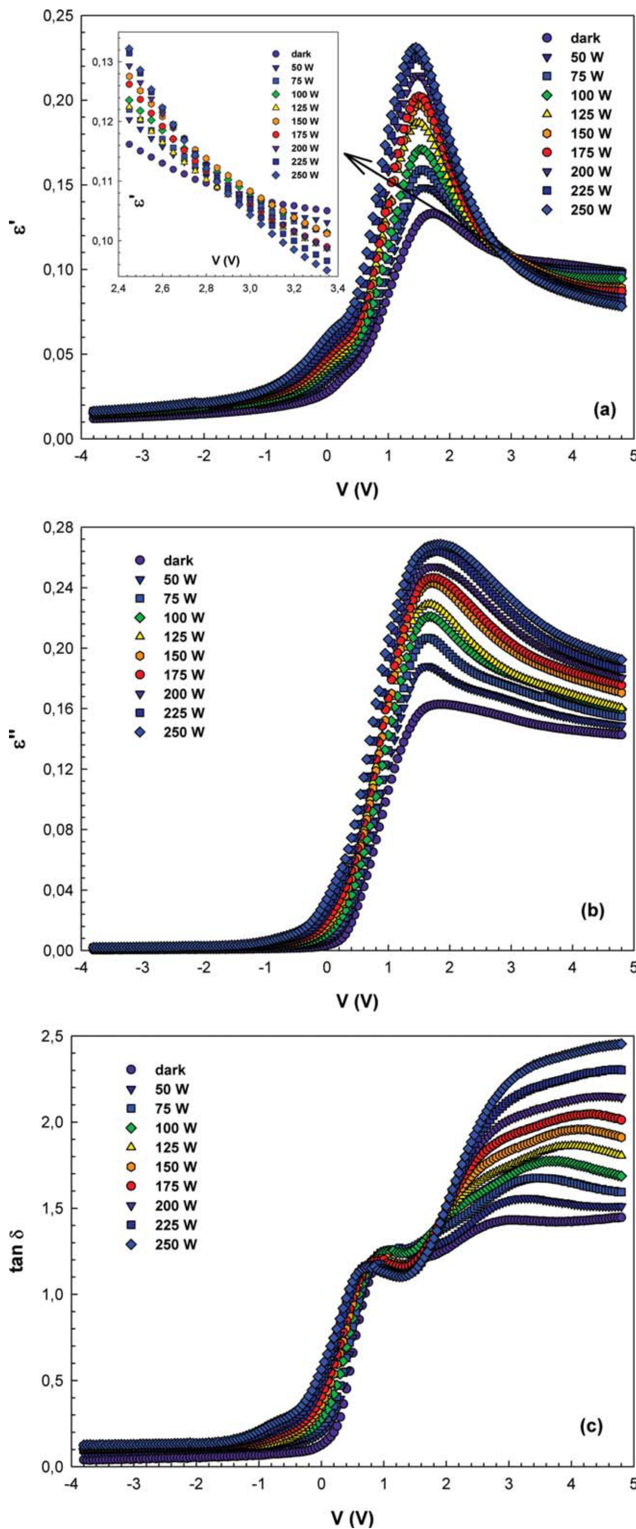

Figure 2 The variations of (a) the dielectric constant ε′ vs. V; (b) dielectric loss ε″ vs. V, and (c) tangent loss tanδ vs. V in dark and under various illumination intensities for Au/PVA (Co, Zn-doped)n-Si SBD. [Color figure can be viewed in the online issue, which is available at wileyonlinelibrary.com.]

almost common intersection point of all the curves at about 2.8 V. At about the intersection point, the value of ε′ is almost independent of the illumination intensity. To show these intersection points with illumination intensity, the ε′–V plots around intersection point were given inset in Figure 2(a). It is clear that the intersection point changes with illumination intensity, but this change in intersection point is not considerable. The crossing of the ε′–V plots shows

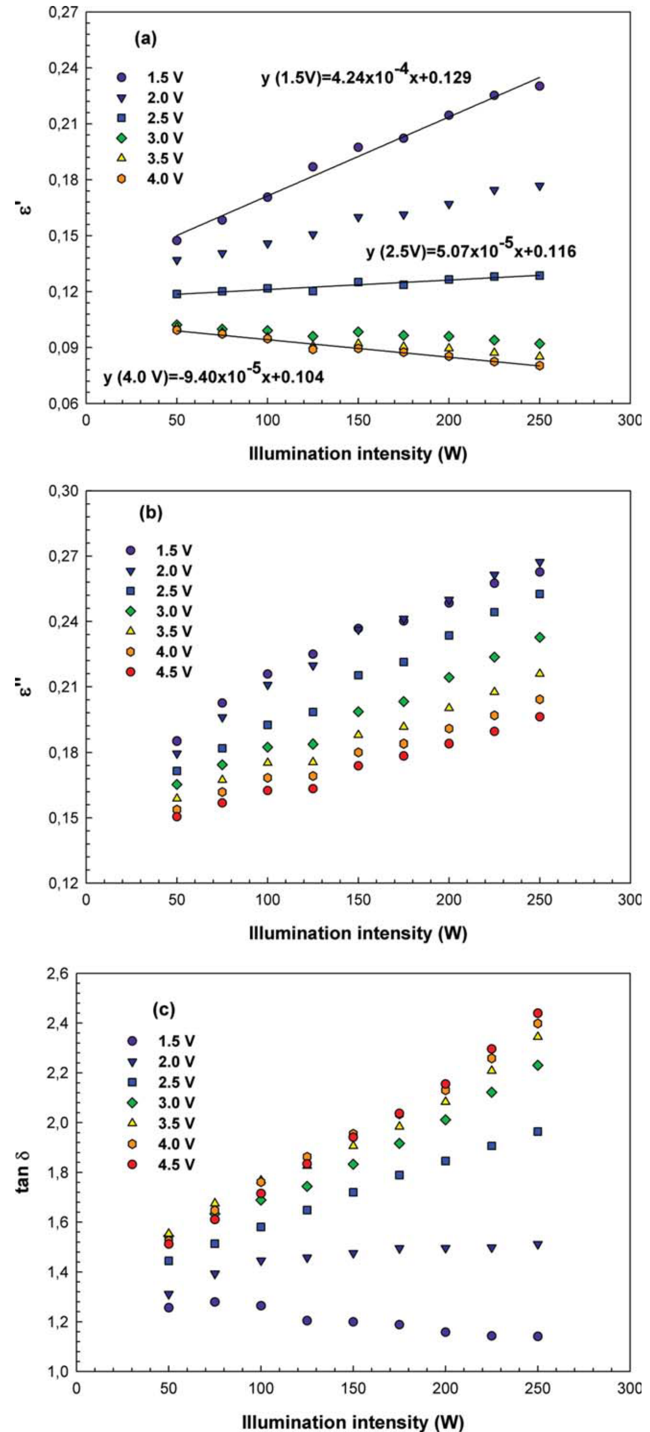

Figure 3 Illumination dependence of the (a) ε′, (b) ε″, and (c) tanδ for various applied voltage of Au/PVA(Co, Zn-doped)/n-Si SBD at room temperature. [Color figure can be viewed in the online issue, which is available at wileyonlinelibrary.com.]

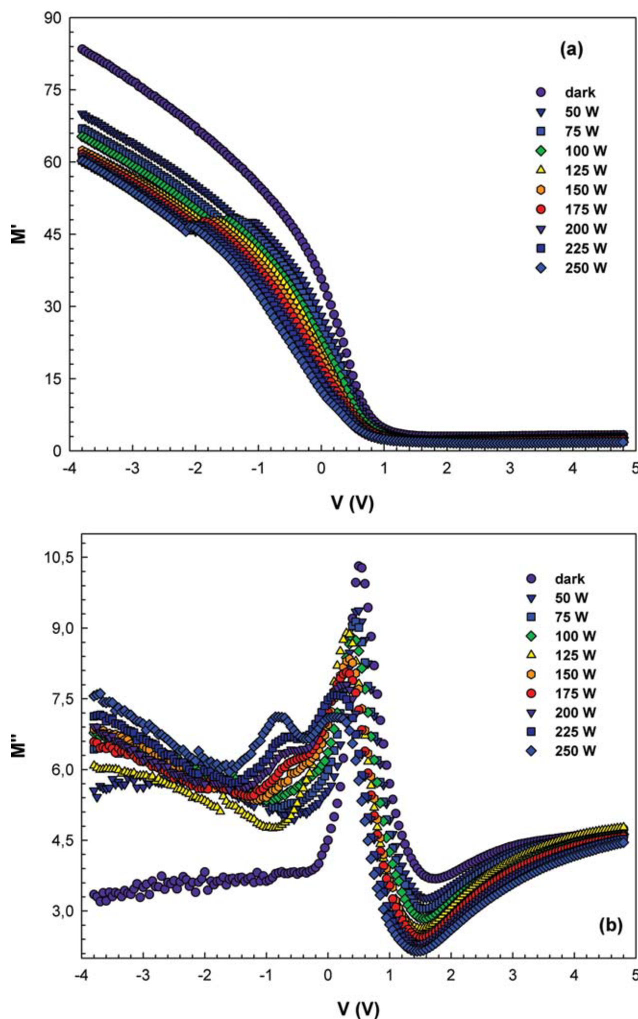

Figure 4 a: The real part M' and (b) the imaginary part M'' of electric modulus M^* vs. V in dark and under various illumination intensities for Au/PVA(Co, Zn-doped)/n-Si SBD. [Color figure can be viewed in the online issue, which is available at wileyonlinelibrary.com.]

an abnormal behavior, when seen with respect to the conventional behavior of ideal Schottky diode, because the value of ε′ decreases with the increasing illumination intensity after the intersection point. There are many reports in the literature about temperature and radiation dependent intersection point of I–V and C–V plots.[34–40] Such behavior of ε′ is mainly attributed to the molecular restructuring and reordering of the interface states (N_{ss}), series resistance (R_s), the inhomogeneties of barrier height (BH), and interfacial layer at M/S interface.[37–42] It is thought that the presence of R_s keeps this intersection behavior hidden and unobservable in homogeneous SBDs, but it appears in the case of inhomogeneous SBDs.[43,44] It is well known that the value of C and G/ω are extremely sensitive to the interface properties and R_s under illumination effect. Also, under illumination, the value of R_s decreases because of the reduction in carrier density in the depletion region of diode through introduction of traps and recombination centers associated with illumination intensity effect. Therefore, intersection behavior in the forward bias ε′–V or C–V plots will be inevitable. These results show that under high illumination intensities, the electronic, ionic, dipolar and interfacial, or surface polarization contribute to the values of ε′ and ε″. In the strong accumulation region [as seen in Fig. 2(a,b)], the values of ε′ become closer to the values of ε″ because in this region the effect of N_{ss} can be eliminated. According to eq. 5, the change in the tanδ–V plots [Fig. 2(c)] thoroughly can be attributed to the change of ε′ and ε″ with illumination intensity. After the intersection, R_s becomes more effective rather than N_{ss}.

The illumination dependency of ε′, ε″, and tanδ of Au/PVA(Co, Zn-doped)/n-Si SBDs at different voltage values is presented in Figure 3(a–c), respectively. It was found that the parameters ε′, ε″, and tanδ obtained from the measured capacitance and conductance are strong

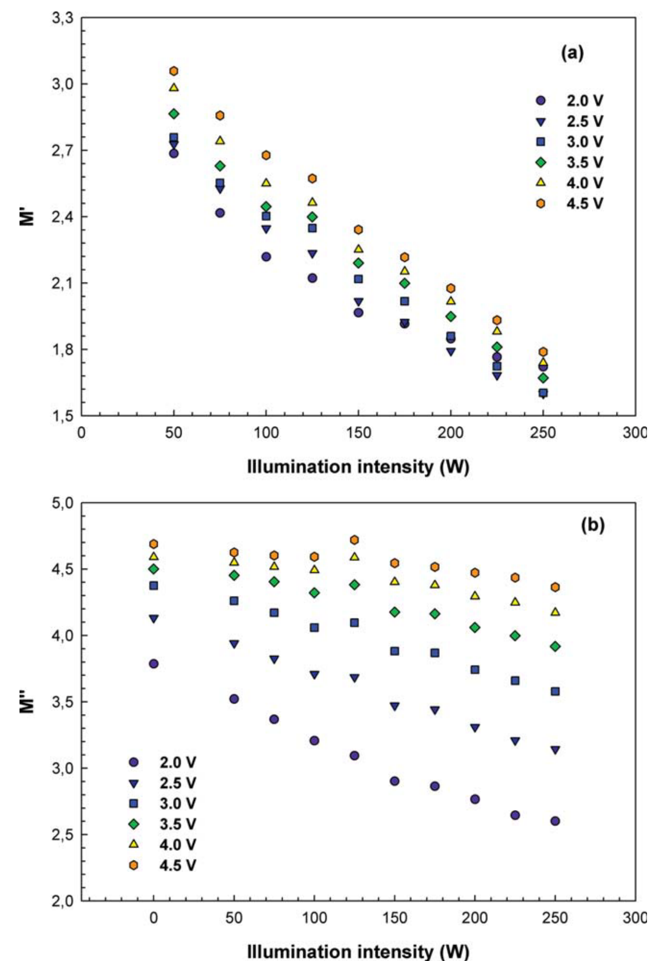

Figure 5 Illumination dependence of the (a) M' and (b) M'' for various applied bias voltage of Au/PVA(Co, Zn-doped)/n-Si SBD at room temperature. [Color figure can be viewed in the online issue, which is available at wileyonlinelibrary.com.]

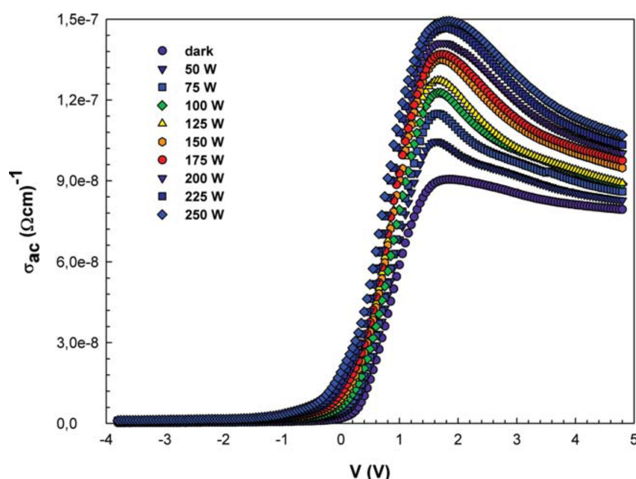

Figure 6 The variation of the AC electrical conductivity σ_{AC} with applied bias voltage in dark and under various illumination intensities for Au/PVA(Co, Zn-doped)/n-Si SBD. [Color figure can be viewed in the online issue, which is available at wileyonlinelibrary.com.]

functions of applied bias voltage, especially at high illumination intensities (P), and they change linearly with illumination. Similar to Figure 2(a), the change in ε' values with P are different before and after intersection point. As can be seen Figure 3(a), the slopes of ε'–P plots are positive before intersection and negative after intersection; whereas, the slopes of ε''–P and tanδ–P plots have positive value.

Figure 4(a,b) shows the applied bias voltage dependency of the real and imaginary parts of complex electric modulus, respectively, for Au/PVA (Co, Zn-doped)n-Si SBDs in dark and under various illumination intensities. As can be seen in these figures, M' and M'' strongly depends on both illumination intensities and applied bias voltage. As shown in Figure 4(b), the M''–V characteristics have a distinctive anomalous peak in the depletion region between 0.1 and 0.5 V in dark and illumination conditions. However, in the inversion region, there is the second broad peak except for in-dark. Such behavior of these two peaks can be attributed to the particular distribution of interface states and they localized in these two regions. In other words, M'reaches a maximum constant value corresponding to $M = 1/\varepsilon_\infty$ due to the relaxation process.

The illumination dependency of the real and imaginary parts of electric modulus (M' and M'') of Au/PVA (Co, Zn-doped)/n-Si SBDs at different voltages are presented in Figure 5(a,b), respectively. It is evident from these figures, for each bias voltage M' and M''decreases with the increasing illumination intensity and changes as linearly with illumination.

Figure 6 shows the variation of the AC electrical conductivity (σ_{AC}) with applied bias voltage (in the illumination range of 0–250 W) at room temperature for Au/PVA(Co, Zn-doped)/n-Si SBDs. It is clear that the value of σ_{AC} increases with the increasing illumination intensities and σ_{AC} vs. V plot gives a peak for each illumination intensity because of the effect of R_s in the accumulation region. As the illumination level is increased, more and more charge accumulation occurs at the polymer–semiconductor interface, which leads to a rise in the conductivity.

Figure 7(a,b) shows the σ_{AC}–P and $\ln(\sigma_{AC}) - 1/P$ plots for various bias voltages in the depletion region at room temperature for Au/PVA(Co, Zn-doped)/n-Si SBDs, respectively. As shown in Figure 7(a), the illumination dependency of the photoconductivity increases with the increasing illumination at each bias voltage and shows a linear behavior. On the other hand, Figure 7(b) shows two distinct illumination regions at each bias voltage. The meaning of such behavior $\ln(\sigma_{AC}) - 1/P$ plot shows two different conduction mechanisms. Increasing the illumination intensity would result in an increase in the number of charge carriers created. The increase in conductivity at high illumination intensity may be caused by the liberation of electrons or ions through the amorphous region of PVA, or probably the internal stresses in the

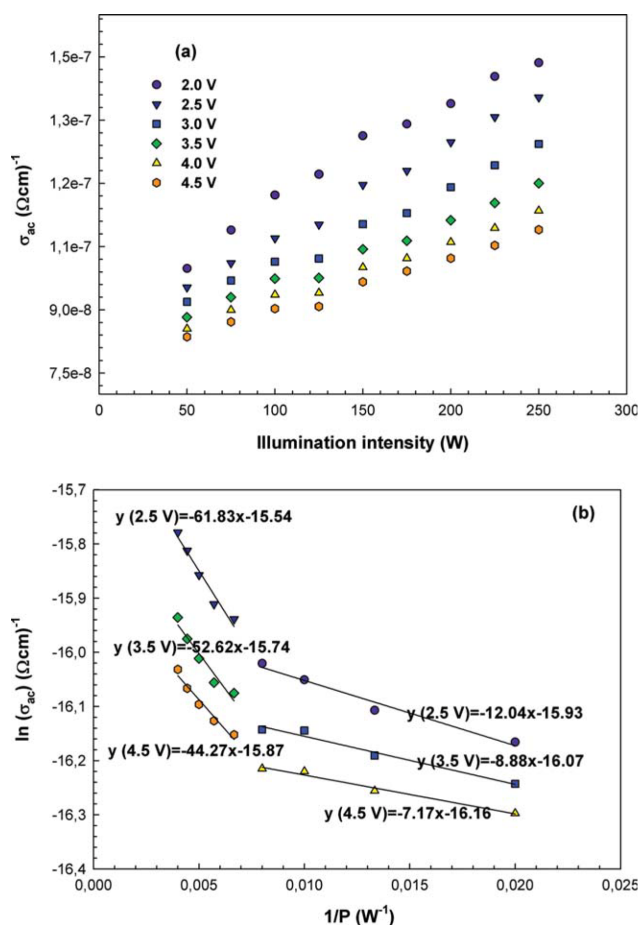

Figure 7 a: Illumination dependence of σ_{AC} vs. P and (b) $\ln(\sigma_{AC})$ vs. $1/P$ plots for various applied voltage of Au/PVA(Co, Zn-doped)/n-Si SBD at room temperature, respectively. [Color figure can be viewed in the online issue, which is available at wileyonlinelibrary.com.]

doped (Co, Zn) sample may also play a role in the motion of charge carriers.[1,43,44]

CONCLUSION

In this study, we have presented and discussed the effects of illumination and applied bias voltage on the main dielectric properties of Au/PVA (Co, Zn-doped)/n-Si SBDs. An analysis of experimental results has shown that the values of dielectric constant (ε'), dielectric loss (ε''), loss tangent (tanδ), the real and imaginary parts of electric modulus (M' and M'') and AC electrical conductivity (σ_{AC}) were found strongly dependent on both the illumination intensity and applied bias voltage especially in depletion and accumulation regions. These changes in dielectric properties were attributed to the molecular restructuring and reordering of N_{ss}, the inhomogeneties of the BH and interfacial polymer layer at M/S interface and R_s of SBDs. The ε'–V plots also show an intersection feature at $\sim$ 2.8 V, and, for this point, the value of ε' is almost independent of the illumination intensity. Such behavior of the ε'–V plots appears as an abnormality compared with the conventional behavior of an ideal SBD. It is believed that the existence of the R_s keeps this intersection hidden and unobservable in homogenous SBDs, but it appears in the case of an inhomogenous SBDs. It is concluded that illumination intensity enhances the conductivity of Au/PVA(Co, Zn-doped)/n-Si SBD.

References

1. Shehap, A.; Abd Allah, R. A.; Basha, A. F.; Abd El-Kader, F. H. J App Poly Sci 1998, 68, 687.
2. Abd El-Kader, F. H.; Hamza, S. S.; Attia, G. J Mater Sci 1993, 28, 6719.
3. Abd El-Kader, F. H.; Attia, G.; Ibrahim, S. S. J Poly Degrad Stab 1994, 43, 253.
4. Lu, X.; Brown, N.; Shaker, M.; Kamel, I. L. J Poly Sci Part B Polym Phys 1995, 33, 153.
5. Taşçıoğlu, İ.; Uslu, H.; Altındal, Ş.; Durmuş, P.; Dökme, İ.; Tunç, T. J App Poly Sci 2010, 118, 596.
6. Nalwa, H. S. J Mat Sci 1992, 27, 210.
7. Farag, A. A. M.; El-Shazly, E. A. A.; Abdel Rafea, M.; Ibrahim, A. Sol Energ Mat Sol C 2009, 93, 1853.
8. Syed Abthagir, P.; Saraswathi, R. Org Electron 2004, 5, 299.
9. Bohler, A.; Dirr, S.; Johannes, H. H.; Ammermann, D.; Kowalsky, W. Synth Met 1997, 91, 95.
10. Yakovlev, Y. O.; Zolin, V. F. Synth Met 1997, 91, 205.
11. Altındal, S.; Sari, B.; Unal, H. I.; Yavas, N. J App Poly Sci 2009, 113, 2955.
12. Zhang, J.; Jiang, F. Chem Phys 2003, 289, 243.
13. Dharmaraj, N.; Kim, C. H.; Kim, H. Y. Synth React Inorg M 2006, 36, 29.
14. Bazuev, G. V.; Gyrdasova, O. I.; Grigorov, I. G.; Koryakova, O. V. Inorg Mat 2005, 41, 288.
15. Guan, H.; Shao, C.; Wen, S.; Chen, B.; Gong, J.; Yang, X. Mat Chem Phys 2003, 82, 1002.
16. Lee, J. S., Choi, K. H.; Ghim, H. D.; Kim, S. S.; Chun, D. H.; Kim, H. Y.; Lyoo, W. S. J App Poly Sci 2004, 93, 1638.
17. Uslu, H.; Şafak, Y.; Taşçıoğlu, İ.; Altındal, Ş. J Optoelectron Adv Mater 2010, 12, 262.
18. Uslu, H.; Altındal, Ş.; Aydemir, U.; Dökme, İ.; Afandiyeva, İ. M. J Alloys Compd 2010, 503, 96.
19. Parveen, A.; Kumar, K. A.; Revanasidappa, M.; Ekhilikar, S.; Prasad, M. V. N. Ferroelectrics 2008, 377, 63.
20. Dökme, İ.; Altındal, Ş.; Tunç, T.; Uslu, I. Microelectron Reliab 2010, 50, 39.
21. Saito, H.; Stuhn, B. Polymer 1994, 35, 475.
22. Popescu, M.; Bunget, I. Physics Solid Dielectrics; Elsevier: Amsterdam, 1984.
23. Akkal, B.; Benamara, Z.; Gruzza, B.; Bideux, L.; Bachir Bouiadjra, N.; Mat Sci Eng C 2002, 21, 291.
24. Symth, C. P. Dielectric Behaviour and Structure; McGraw-Hill: New York, 1955.
25. Daniel, V. V. Dielectric Relaxation; Academic Press: London, 1967.
26. Pissis, P.; Kyritsis, A. Solid State Ionics 1997, 97, 105.
27. Dökme, İ.; Altındal, Ş.; Gökçen, M. Microelectron Eng 2008, 85, 1910.
28. Pakma, O.; Serin, N.; Serin, T.; Altındal, Ş. J Phys D Appl Phys 2008, 41, 215103.
29. Chelkowski, A. Dielectric Physics; Elsevier: Amsterdam, 1980.
30. Mattsson, M. S.; Niklasson, G. A.; Forsgren, K.; Harsta, A. J Appl Phys 1999, 85, 2185.
31. Prabakar, K.; Narayandass, S. K.; Mangaralaj, D. Phys Status Solidi B 2003, 199, 507.
32. Macedo, P. B.; Moyniham, C. T.; Bose, R. Phys Chem Glass 1972, 13, 171.
33. Afandiyeva, İ. M.; Dökme, İ.; Altındal, Ş.; Bülbül, M. M.; Tataroğlu, A. Microelectron Eng 2008, 85, 247.
34. Taşçıoğlu, İ.; Tataroğlu, A.; Özbay, A.; Altındal, Ş. Radiat Phys Chem 2010, 79, 457.
35. Altındal, Ş.; Kanbur, H.; Yücedağ, İ.; Tataroğlu, A. Microelectron Eng 2008, 85, 1495.
36. Chattopadhyay, P.; Raychaudhuri, B. Solid State Electron 1993, 36, 605.
37. Chattopadhyay, P.; Raychaudhuri, B. Solid State Electron 1992, 35, 875.
38. Bülbül, M. M.; Zeyrek, S.; Altındal, Ş.; Yüzer, H. Microelectron Eng 2006, 83, 577.
39. Ho, P. S.; Yang, E. S.; Evans, H. L.; Wu, X. Phys Rev Lett 1986, 56, 177.
40. Pakma, O.; Serin, N.; Serin, T.; Altındal, Ş. Semicond Sci Tech 2008, 23, 105014.
41. Chand, S. Semicond Sci Tech 2004, 19, 82.
42. Osvald, J. Solid State Electron 2006, 50, 228.
43. Hogarth, C. A.; Bosha, M. J. J Phys D Appl Phys 1983, 16, 869.
44. Muralidhar, C.; Pillai, P. K. C. J Mat Sci Lett 1987, 6, 439.